# Cellulose Nanowhiskers and Fiber Alignment Greatly Improve Mechanical Properties of Electrospun Prolamin Protein Fibers

Yixiang Wang and Lingyun Chen*

Department of Agricultural, Food and Nutritional Science, University of Alberta Edmonton, Alberta, Canada T6G 2P5

ABSTRACT: Electrospun fibers from natural polymers must possess appropriate mechanical properties if they are to be functional in numerous applications. In this research, two convenient physical approaches were applied to reinforce the assembled hordein/zein electrospun nanofabrics: incorporation of surface-modified cellulose nanowhiskers (SCN) and fiber alignment. The mechanical properties and stability of the modified fibers were tested in relation to fiber morphology and structure as characterized by scanning electron microscopy, transmission electron microscopy, Fourier-transform infrared spectroscopy, and Raman spectroscopy. SCN modified by quaternary ammonium salt were well-dispersed in hordein/zein networks, leading to fibers with significantly improved mechanical properties and water resistance. With the addition of 3 wt % SCN, the tensile strength and Young's modulus of hordein/zein fibers increased from 4.36 ± 0.29 to 7.79 ± 0.36 MPa and from 195.80 ± 13.02 to 396.64 ± 18.33 MPa, respectively, and the elongation at break was retained because of the formation of a percolating network of SCN. The alignment of electrospun fibers strengthened the hordein/zein nanofabrics in both tangential and normal directions to 17.26 ± 1.41 and 14.02 ± 0.74 MPa, respectively, by not only altering the piling up pattern, but also by promoting phase separation and improved interactions. When applying both of the reinforcing methods, the tensile strength of hordein/zein fibers was further enhanced to 21.99 ± 1.19 MPa, stronger than that of cancellous bones (5−10 MPa). All the reinforced fibers exhibited a reduced burst effect in phosphate-buffered saline (PBS) while releasing the incorporated bioactive molecule in a controlled manner. These physically reinforced prolamin protein fibers possessed significantly improved mechanical properties and may have potential to be used as tissue engineering scaffold materials or natural delivery systems for biomedical applications.

KEYWORDS: prolamin proteins, electrospun fibers, reinforcement, surface modified cellulose nanowhiskers, alignment
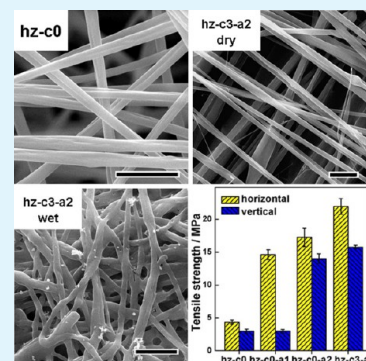
1. INTRODUCTION

Electrospun submicrometer/nanofibers possess a very large surface area to volume ratio and an excellent pore interconnectivity. These attributes confer novel and significantly improved properties,[1] and so have attracted a tremendous amount of attention over the past few decades for their potential in broad applications such as filtration, affinity membranes, recovery of metal ions, tissue engineering scaffolds, wound healing, drug release, catalyst and enzyme carriers, sensors, energy storage, etc.[2,3] Proteins are fundamental building blocks of life, playing an essential role in motility, elasticity, scaffolding, stabilization and protection of cells, tissues and organisms.[4] Electrospun fibers made of protein are then especially interesting for biomedical field applications; however, most electrospun protein fabrics suffer from the poor tensile strength and water resistance.[5,6] Limited recent research reports the physical and chemical approaches to reinforce electrospun protein fibers. For example, multiwalled carbon nanotubes (MWNT) have been incorporated in silk fibroin fibers to drastically enhance their mechanical properties. The composite fibers with 1 wt % MWNT exhibited the highest breaking strength, Young's modulus and breaking energy of 3.24 ± 0.27 MPa, 191.70 ± 12.80 MPa, and 29.28 ± 6.68 J kg^{-1}, respectively.[7] On the other hand, glyoxal and

glutaraldehyde have been used as the cross-linking reagents to produce zein fibers with improved solvent resistance.[8,9] More research is required to develop viable techniques to make affordable electrospun protein fabrics with good performance.

Cellulose nanowhiskers, usually obtained by acid hydrolysis of native cellulose,[10] are good candidates to be natural reinforcing elements in composites because of their very large surface to volume ratio, high surface area, good mechanical properties, renewability, low cost, and easy chemical and mechanical modification. A new and convenient method has recently been developed to prepare anionically charged cellulose nanowhiskers without using intensive treatments, such as mechanical shear or ultrasound traditionally required to disperse cellulose.[11] Nanowhiskers can be further modified by absorbing quaternary ammonium salts on the surface so as to be well-dispersed in organic solvents.[12] These rodlike nanowhiskers with a high bending strength of about 10 GPa and high Young's modulus of approximately 150 GPa, have a large tendency to form networks which is favorable to the formation of load-bearing percolating architectures within the host

Table 1. Various Components and Collecting Manner of Electrospun Hordein/Zein/SCN Fibers

sample	solution components				solution volume for each layer (mL)		
	hordein (g)	zein (g)	SCN (g)	acetic acid (mL)	random	tangential	normal
hz-c0	0.378	0.162	0	3	3		
hz-c1			0.0054		3		
hz-c3			0.0162		3		
hz-c5			0.027		3		
hz-c0-a1			0		1.5	1.5	
hz-c0-a2			0			1.5	1.5
hz-c0-a3			0		1	1	1
hz-c3-a2			0.0162			1.5	1.5

polymer matrix.[13,14] Currently, cellulose nanowhiskers have been successfully used as reinforcing fillers in a series of membranes and hydrogels,[15,16] but only a few examples show their application in strengthening electrospun protein fabrics.[17]

Also, it has been demonstrated that the alignment of electrospun fibers could endow them with better properties than those of randomly oriented ones.[18] Lee and Deng recently fabricated aligned poly (vinyl alcohol) (PVA) electrospun fiber webs which showed high modulus and tensile strength along the fiber direction compared with isotropic PVA webs.[19] Similar results were reported where the application of an electrostatic and centrifugal field improved the degree of uniaxial alignment in polymer nanofibers and enhanced orientational order in polymer chains, producing bisphenol A polycarbonate (BPAPC) nanofiber with superior mechanical properties.[20] However, this technology has seldom been used for preparing plant-protein-based fibers.

To support the agriculture and food industries, improved utilization of the coproducts from the industrial processing of cereal crops is important. Zein and hordein are the major storage proteins in corn and barley, respectively, and are largely available as the byproducts of starch or beta-glucan processing; however, currently they are not being fully utilized. In our previous work, electrospun-assembled prolamin protein fibers with hydrophobic zein particles as the filler and flexible hordein molecules as the matrix were successfully prepared. These fibers showed promise as three-dimensional delivery vehicle of bioactive compounds.[21] To further improve their mechanical properties and expand their applications, phenyltrimethylammonium chloride was used in this study to modify cellulose nanowhiskers (SCN), and these were dispersed in hordein/zein acetic acid solutions as hydrophobic rigid fillers to prepare electrospun fibers. Meanwhile, varying rotating speeds and collecting directions were used to build three kinds of orientated fabrics. The effects of SCN content and alignment on the morphology, structure and properties of electrospun hordein/zein fibers are discussed. In addition, their controlled release profile was evaluated in the simulated human body fluid.

2. EXPERIMENTAL METHODS

2.1. Materials. Zein (F4000, protein content of 92%, approximate molecular weight of 35 000 Da, and total ash of 2%) was purchased from Freeman Industries LLC (New York, NY, USA) and used without further purification. Regular barley grains (Falcon) were kindly provided by Dr. James Helm, Alberta Agricultural and Rural Development, Lacombe, Alberta. Barley protein content was 13.2 wt % (dry status) as determined by combustion with a nitrogen analyzer (FP-428, Leco Corporation, St. Joseph, MI, USA) calibrated with analytical reagent grade EDTA (a factor of 6.25 was used to convert the nitrogen to protein). Hordein (total ash of 2%) was extracted using the alcohol method according to our previous work, and the

protein content (dry status) was 92 wt % as determined by the same nitrogen analyzer.[22] Bleached kraft pulp (Alpac spruce, Alberta-Pacific Forest Industries Inc., AB, Canada) with 87.3% α-cellulose and 13.6% hemicellulose was used as cellulose material. Its viscosity-average molecular weight (M_η) was determined with an Ubbelohde viscometer in LiOH/urea aqueous solution at 25 ± 0.1 °C and calculated to be 4 $\times 10^5$ Da. Sodium (meta) periodate (NaIO$_4$), sodium chlorite (NaClO$_2$, 80% purity), sodium hypochlorite solution (NaClO, 10−15% available chlorine), 2,2,6,6-tetramethylpiperidinyl-1-oxyl (TEMPO), phenyltrimethylammonium chloride (97%), and riboflavin were purchased from Sigma-Aldrich Canada Ltd. (Oakville, ON, Canada). Acetic acid and all other chemical reagents were purchased from Fisher Scientific (Markham, ON, Canada) and were used as received unless otherwise described.

2.2. Preparation and Surface Modification of Cellulose Nanowhiskers. Cellulose nanowhiskers with many anionic groups (containing 3.5 mmol/g carboxyl groups) were prepared as described by van de Ven et al.[23] Briefly, bleached kraft pulp was oxidized by NaIO$_4$ in NaCl aqueous solution at room temperature for 36 h. Then, NaClO$_2$ and H$_2$O$_2$ were added to the mixture, and the pH was maintained at 5 by adding 0.5 M NaOH. After another 24 h, the suspension was poured into ethanol to obtain a white precipitate, which was thoroughly washed with water−ethanol solution, followed by acetone, and dried in a fume hood. The chlorite-oxidized cellulose pulp was further reacted with TEMPO at 60 °C for 48 h to get negatively charged cellulose nanowhiskers (CN). CN was subsequently modified using phenyltrimethylammonium chloride as model positively charged molecule as described by Salajková et al to achieve good dispersion in an organic solvent.[12] The CN aqueous suspension was adjusted to pH 10 and then added into phenyltrimethylammonium chloride solution. The mixture was kept at 60 °C for 3 h and then stirred at room temperature overnight. The resultant suspension was dialyzed against deionized water and freeze-dried to obtain the surface modified cellulose nanowhiskers (SCN). The morphology of CN and SCN was observed on a JEM-2200 TEM (JEOL TEM, Japan). CN and SCN were dispersed in water and acetic acid, respectively. A small droplet of dilute suspension was then deposited on a polycarbon film supported on a copper grid, and a thin layer was suspended over the holes of the grid. The specimen was dried in air at ambient pressure, and then was imaged on TEM at an accelerating voltage of 80 kV.

2.3. Randomly Orientated and Aligned Electrospun Hordein/Zein/SCN Fibers. The sample components and collecting manner are listed in Table 1. The hordein/zein ratio of 7:3 optimized in our previous work was chosen.[21] Briefly, 0.378 g of hordein, 0.162 g of zein, and desired amounts of SCN were blended in a mortar, and then dispersed in 3 mL of pure acetic acid. The solutions were allowed to stir at room temperature for 4 h. To understand the variation in structure of different hordein/zein/SCN composite solutions, they were characterized with respect to their complex viscosity by a DHR-3 rheometer (TA Instruments, DE, USA) fitted with a cylinder measuring system. The sweep of the frequency was from 0.1 to 100 rad/s at 25 °C. Hordein/zein/SCN ultrafine fibers were subsequently fabricated by a customized digital electrospinning apparatus EC-DIG (IME Technologies, Eindhoven, Netherlands) at room temperature. The above prepared solutions were forced through a blunt needle with

a diameter of 0.8 mm at the rate of 1.6 mL h^{-1}, and the applied voltage was fixed at 15 kV. A rotating drum with a diameter of 10 cm was chosen as the collector, and the distance between the tip and collector was set at 15 cm. Rotating speeds of 1 and 2000 rpm were used to prepare randomly oriented and uniaxially aligned electrospun fibers, respectively. Random hordein/zein/SCN composite fibers were coded as hz-c0, hz-c1, hz-c3, and hz-c5, corresponding to a SCN content (based on the total hordein/zein content) of 0, 1, 3, and 5 wt %, respectively. Three kinds of aligned hordein/zein fabrics were then obtained by combining randomly, tangentially, and normally orientated layers in order to investigate the effect of orientations on the tensile strength of resultant fabrics. For example, to prepare hz-c0-a3, we first electrospun 1 mL of hordein/zein solution and collected it at a rotating speed of 1 rpm to form a randomly oriented layer. Then, electrospinning of another 1 mL of hordein/zein solution was collected at a speed of 2000 rpm as the second layer, and this was marked as the tangential direction. The third layer was made from 1 mL of hordein/zein solution and subsequently collected at a speed of 2000 rpm, which was perpendicular to the second layer and marked as the normal direction. Similarly, hz-c0-a1 was prepared by collecting a randomly oriented layer from 1.5 mL of hordein/zein solution and then a uniaxially aligned layer from another 1.5 mL of solution, whereas hz-c0-a2 and hz-c3-a2 were composed of two uniaxially aligned layers orientated in tangential and normal directions, respectively. The total hordein/zein content in each sample was constant.

2.4. Fiber Morphology. Morphology observations of electrospun fibers were carried out with a Philips XL-30 scanning electron microscope (SEM) at an acceleration voltage of 5−10 kV. The samples were vacuum-dried for 24 h and then removed from the fabric with the support of aluminum foil. They were sputtered with gold for 2 min prior to observation and photographing. In the SEM photos, fiber diameters were determined with the ImageJ image-visualization software developed by the National Institute of Health.[24] Two hundred random positions were selected and measured for each sample.

2.5. Structures of Electrospun Fibers. TEM observation of electrospun fibers was carried out to evaluate the dispersion of SCN and phase separation in the hordein/zein matrix. The fibers were embedded in Spurr resin and cured at 70 °C overnight. They were trimmed with a razor blade and then with an ultracut microtome equipped with a glass knife, to obtain an extremely smooth trapezoidal cross-sectional surface. An ULTRACUT E microtome was used for ultrathin microtomy. The top layer (about 1 mm) was first removed using a glass knife, then, ultrathin sections of about 100 nm thickness were cut with a diamond knife at room temperature with unstained samples mounted on 300 mesh Cu/Pd grids. Some ultrathin sections were stained by OsO$_4$ vapor for 18 h and they were finally examined on TEM operating at an accelerating voltage of 80 kV.

FTIR spectra of the electrospun fibers were recorded on a Nicolet 6700 spectrophotometer (Thermo Fisher Scientific Inc., MA, USA). The samples were vacuum-dried for 24 h and then placed on an attenuated total reflectance (ATR) accessory equipped with a Ge crystal. Spectra were recorded as the average of 256 scans at 2 cm^{-1} resolution and 25 °C, using the empty accessory as blank. During measurements the accessory compartment was flushed with dry nitrogen. For the study of the amide I region of the proteins, ATR correction and Fourier deconvolution were performed using the software provided with the spectrometer (Omnic 8.1 software). Fourier self-deconvolution was applied in order to narrow finer bands hidden in larger bands. Parameters used for deconvolution with an enhancement of 2 and bandwidth of 20 cm^{-1}.

Raman spectra of the electrospun fibers were recorded at room temperature using a Renishaw Invia Raman microscope system (Apply Innovation, Gloucestershire, UK) with a laser at 785 nm to avoid excessive fluorescence in the Raman signal. A short working distance 100× objective was used, which under high confocal conditions provided a lateral resolution of about 1 μm and a depth resolution of about 2 μm. Each spectrum was collected by coadding 500 scans, and then baseline-corrected, smoothed by a nine-point Savitzky-Golay

procedure using Origin 8.0,[25] and normalized to the 1450 cm^{-1} peak, previously assigned to an asymmetric methyl deformation, because its intensity appears to be conformation-independent.[26,27] The signal intensity at 1670 cm^{-1} was used to construct the Raman images.

2.6. Fiber Mechanical Properties and Thermal/Solvent Resistance. Tensile testing of the electrospun fibers was done using an Instron 5967 universal testing machine (Instron Corp., MA, USA) at a crosshead speed of 5 mm min^{-1} and a gauge length of 10 mm according to the ASTM D-638-V standard.[28] Five bars with a dimension of 5 cm × 5 mm × 0.1 mm (length × width × thickness) were cut from each fabric mat along tangential and normal directions, respectively. Before testing, the samples were vacuum-dried for 24 h and then allowed to rest for one week in 65% RH. A thermogravimetric analyzer (TGA Q500, TA Instruments, USA) was used to measure the weight loss of fibers in the temperature range from 50 to 550 °C with a heating rate of 10 °C min^{-1} and under an argon gas stream. The water resistance of hordein/zein/SCN fibers was evaluated by immersing the fibers in water bath for 24 h at room temperature. The resultant samples were frozen in liquid nitrogen and freeze-dried for SEM observation.

2.7. Controlled Release. Riboflavin was selected as a bioactive molecule model to investigate the release properties of electrospun hordein/zein/SCN fibers. Drug-loaded fibers were prepared by dispersing riboflavin in hordein/zein/SCN solutions before electrospinning and the riboflavin content was 5 wt % in the final electrospun fibers. The release kinetics was assessed in phosphate-buffered saline (PBS, pH 7.4) with a 2100C dissolution system (Distek Inc., NJ, USA). Riboflavin-loaded fibers (40 mg) were placed into 50 mL of PBS at 37 °C and stirred at 100 rpm. The riboflavin content in the release mediums was monitored with S-3100 UV−vis spectrophotometer (Scinco Co. Ltd., Japan) at a wavelength of 445 nm.

2.8. Statistical Analysis. Experimental results were represented as the mean of five batches ± SD. Statistical evaluation was carried out by analysis of variance (ANOVA) followed by multiple-comparison tests using Duncan's multiple-range test at the 95% confidence level. All of the analyses were conducted using SAS statistical software (SAS Institute, Inc., Cary, NC) with a probability of $p < 0.05$ considered to be significant.

3. RESULTS AND DISCUSSION

3.1. Orientated Hordein/Zein/SCN Structure Characterizations. *3.1.1. CN and SCN Morphology.* The dispersion of nanowhiskers in the matrix greatly affects the reinforcement, so nanowhiskers are usually blended with the suitable polymer solutions to achieve the homogeneous distribution. The morphology of CN and SCN in water and acetic acid is shown in Figure 1. Rodlike CN with uniform dimension exhibited a good dispersion in water due to its large amount of anionic charge groups.[11] However, CN could not form a good suspension in acetic acid, which was the common solvent of hordein and zein. With the addition of quaternary ammonium
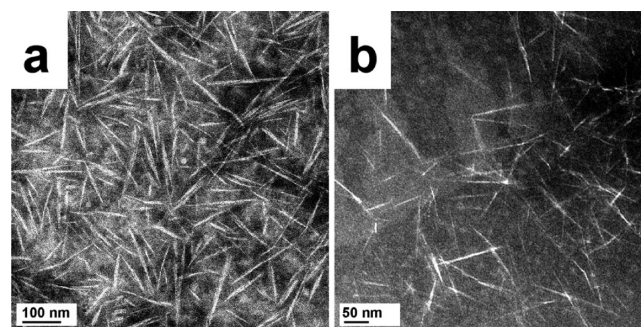

Figure 1. TEM images of (a) CN in water; and (b) SCN in acetic acid at 25 °C.

salt as model positively charged molecule, phenyltrimethylammonium groups were absorbed on the surface of CN to endow it the ability to be dispersed and individualized in an organic solvent.[12] The length (L) and diameter (d) of SCN were 95.92 ± 12.46 and 3.41 ± 0.48 nm, respectively. The average aspect ratio, L/d, was 28.13, which was higher than CN from cotton linter pulp (15) but much lower than the ones from tunicate (70).[16,29] The dimensions of CN varied depending on the raw materials and the physical and chemical treatments performed during the preparation.

3.1.2. Hordein/Zein/SCN Solution Behavior. To investigate the effect of SCN content on hordein/zein network structure in acetic acid solutions, we tested the complex viscosity of each solution. Figure 2 shows the linear viscoelastic frequency sweep
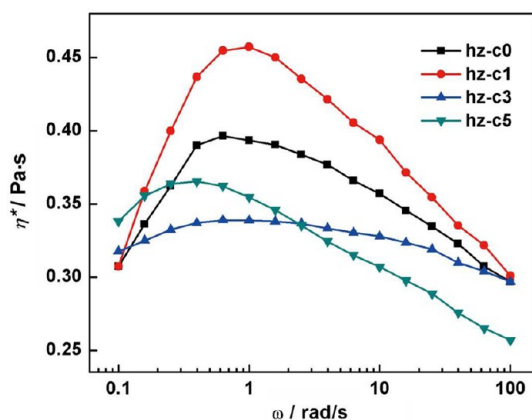
Figure 2. Dependence of complex viscosity on the angular frequency for various hordein/zein/SCN blends in acetic acid at 25 °C.

response of different hordein/zein/SCN solutions. For hz-c0, the sample without addition of SCN, its viscosity increased with shear rate at the very low shear rate region and then decreased when the shear rate was higher than 0.6 rad/s. As revealed in our previous work, an assembled hordein/zein structure was formed with extended hordein molecules acting as the matrix and compact zein particles playing as the filler.[21] Thus, the first segment where the viscosity increased was likely due to the formation of a shear-induced hordein/zein network, and the subsequent decrease in viscosity was caused by the high rate of disruption of the assembled structure, exceeding the rate of reforming new connections. The volume fraction ϕ of SCN in solution to transit from dilute to semi dilute concentration was then calculated by[30]

$$\phi = (\pi/4)(d/L)^2 \tag{1}$$

A ϕ value of 1.59 mg mL^{-1} was obtained by using the density of SCN as 1.60 g/cm^3.[31] The SCN content in hz-c1 solution (1.80 mg mL^{-1}) was near the transition concentration (1.59 mg mL^{-1}) where SCN could barely contact each other. The variation of viscosity of hz-c1 was similar to that of hz-c0, but a much higher peak value was observed at the shearing rate of 1 rad/s. This suggests that the addition of SCN significantly strengthened the hordein/zein composite structure when SCN was separately inserted and wrapped in protein network, and is reflected by the increased viscosity of solution and the higher shearing rate required for composite structure disruption. The complex viscosity exhibited slight changes with shear rate rising when the SCN content was 5.40 mg mL^{-1} in hz-c3. This was probably due to a significantly higher SCN content than the

transition concentration, which provided them more opportunities to interact, not only with protein molecules, but also with each other. These connections may have blocked the formation of a hordein/zein network, because the complex viscosity was obviously reduced even compared to that of hz-c0 at the shearing rate of 1 rad/s. With the addition of 5 wt % SCN, the complex viscosity of the composite solution decreased rapidly when the shear rate was higher than 0.4 rad/s. This suggests that the rate to reform new connections between extended hordein molecules under shearing was obviously reduced by incorporating a large amount of SCN. From above data, the amount of SCN dispersed in hordein/zein solutions significantly impacted the protein network structure formation, and thus could alter the properties of assembled fibers.

3.1.3. Fiber Morphology. Figure 3 shows the SEM images of orientated electrospun hordein/zein/SCN fibers, and their
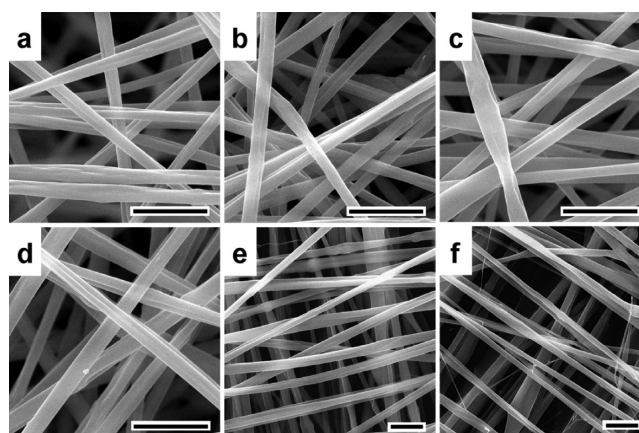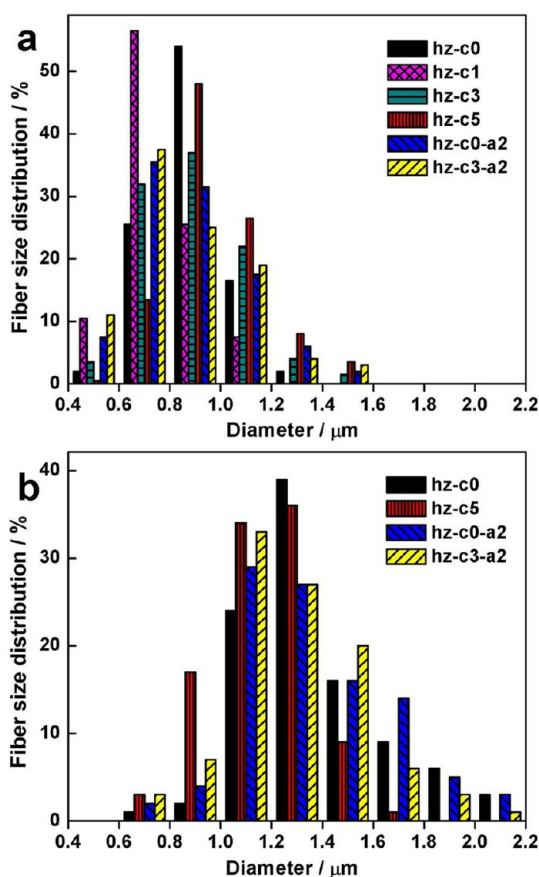
Figure 3. SEM images of orientated electrospun hordein/zein/SCN fibers: (a) hz-c0, (b) hz-c1, (c) hz-c3, (d) hz-c5, (e) hz-c0-a2, and (f) hz-c3-a2. Scale bar: 5 μm.

diameter distribution is summarized in Figure 4a. All the samples exhibited a smooth surface and uniform size, suggesting a well-maintained electrospinnability after the addition of SCN and a good dispersion of SCN in hordein/zein network. Log-normal function D has been used to describe the size-distribution of objects like fibers[32]

$$D = A\exp[-(\ln(x) - \ln(m))^2/s^2] \tag{2}$$

where m is the mode and s^2 is the variance. All diameter distributions were properly fitted ($R^2 = 0.902-0.996$), and the parameters m and s^2 were listed in Table 2. Number average diameters (d_n) and diameter-weighted average values (d_l) were calculated as well. The diameter polydispersity indexes can be therefore defined as $P_d = d_l/d_n$. No significant differences were observed among the diameters of different samples. Compared to that of hz-c0, the d_n value of hz-c1 slightly decreased from 880 to 760 nm; however, with the further addition of SCN, the d_n values mildly increased to 900 and 980 nm for hz-c3 and hz-c5, respectively. Adequate interactions between the protein molecules are required for the formation of continuous fibers during electrospinning.[33] When the amount of rodlike SCN was low, it could insert into hordein/zein network to strengthen the assembled structure, which provided extra connections between protein molecules and facilitated the formation of electrospun fibers with smaller diameters. As the

Figure 4. Diameter distribution of orientated electrospun hordein/zein/SCN fibers: (a) dry status, and (b) immersed in water for 24 h.

3.1.4. Fiber Structure. The unstained section of hz-c3-a2 was examined by TEM and the annular dark field (ADF) image is shown in Figure 5a. ADF-TEM is a promising technique for
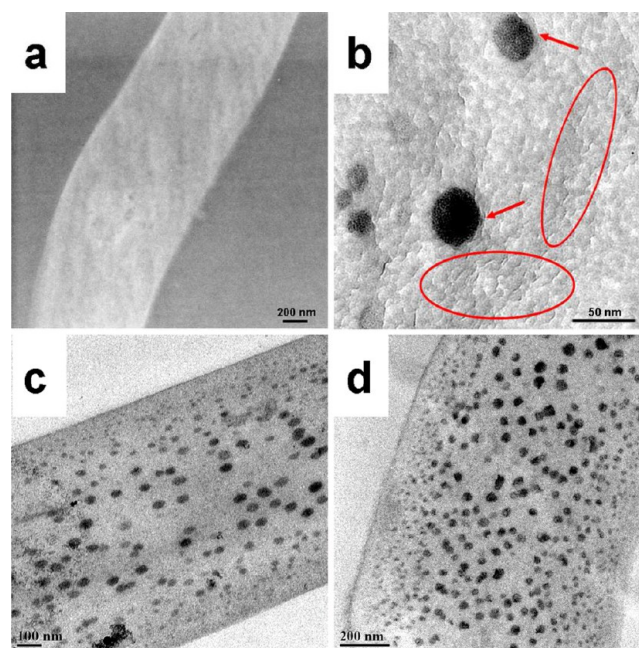

Figure 5. TEM images of ultrathin sections of (a) unstained hz-c3-a2, (b) hz-c3-a2 stained by OsO$_4$, (c) hz-c0 stained by OsO$_4$, and (d) hz-c0-a2 stained by OsO$_4$.

SCN content increased, it not only reinforced the hordein/zein network, but also gradually blocked the combination of protein molecules, leading to slightly enlarged fibers. The P_d values did not change with the addition of SCN, which further proved that SCN was uniformly dispersed in hordein/zein network. To evaluate the effect of uniaxial alignment on the diameter distribution of electrospun hordein/zein/SCN fibers, the morphology of hz-c0-a2 without SCN and hz-c3-a2 with SCN was also observed. As shown in images e and f in Figure 3, the alignment in two directions was achieved, where fibers were parallel piled up. The d_n values of hz-c0-a2 and hz-c3-a2 were similar to that of hz-c0, although their P_d values slightly increased and some thinner fibers were observed that may be caused by stretching of fiber along the aligned axis. Therefore, both aligned and random hordein/zein/SCN fibers were successfully fabricated without significant change of fiber size and morphology.

electron tomography because the recorded image is a chemically sensitive projection of the crystal structure with an advantage of reduced signal noise.[34] It has been proven that SCN exhibited a typical diffraction pattern of cellulose I,[12] so the dispersion of SCN in hordein/zein network could be revealed in the ADF image. Continuous gray shadows existed in hz-c3-a2 fiber and no dark spots could be distinguished, indicating the uniform dispersion of SCN. As shown in Figure 5b, the SCN was individually and randomly embedded in the prolamin protein matrix and formed the continuous filler network when the SCN content was 3 wt %. It directly demonstrates that SCN can be well-dispersed in acetic acid and then homogeneously incorporated into electrospun hordein/zein fibers as potential reinforcing fillers. However, the distribution of SCN was not obviously altered by the alignment of fibers. The section of hz-c0 and hz-c0-a2 was subsequently stained by OsO$_4$ vapor to further investigate the effect of alignment on the inner structure of orientated fibers. Osmium is highly electropositive with an initial oxidation state of +8 and

Table 2. Diameters of Orientated Electrospun Hordein/Zein/SCN Fibers at Dry Status and Immersed in Water for 24 h^a

	dry status					immersed in water for 24 h				
sample	m (μm)	s^2	d_n (μm)	d_l (μm)	P_d	m (μm)	s^2	d_n (μm)	d_l (μm)	P_d
hz-c0	0.86	0.05	0.88 ± 0.14	0.91	1.03	1.26	0.04	1.36 ± 0.27	1.42	1.04
hz-c1	0.71	0.08	0.76 ± 0.14	0.79	1.04	n.d.	n.d.	n.d.	n.d.	n.d.
hz-c3	0.83	0.07	0.90 ± 0.21	0.94	1.04	n.d.	n.d.	n.d.	n.d.	n.d.
hz-c5	0.92	0.06	0.98 ± 0.18	1.01	1.03	1.15	0.06	1.16 ± 0.21	1.20	1.03
hz-c0-a2	0.78	0.14	0.86 ± 0.21	0.92	1.07	1.24	0.09	1.38 ± 0.34	1.46	1.06
hz-c3-a2	0.75	0.16	0.86 ± 0.25	0.93	1.08	1.21	0.07	1.29 ± 0.25	1.34	1.04

^{a}n.d.: not determined.
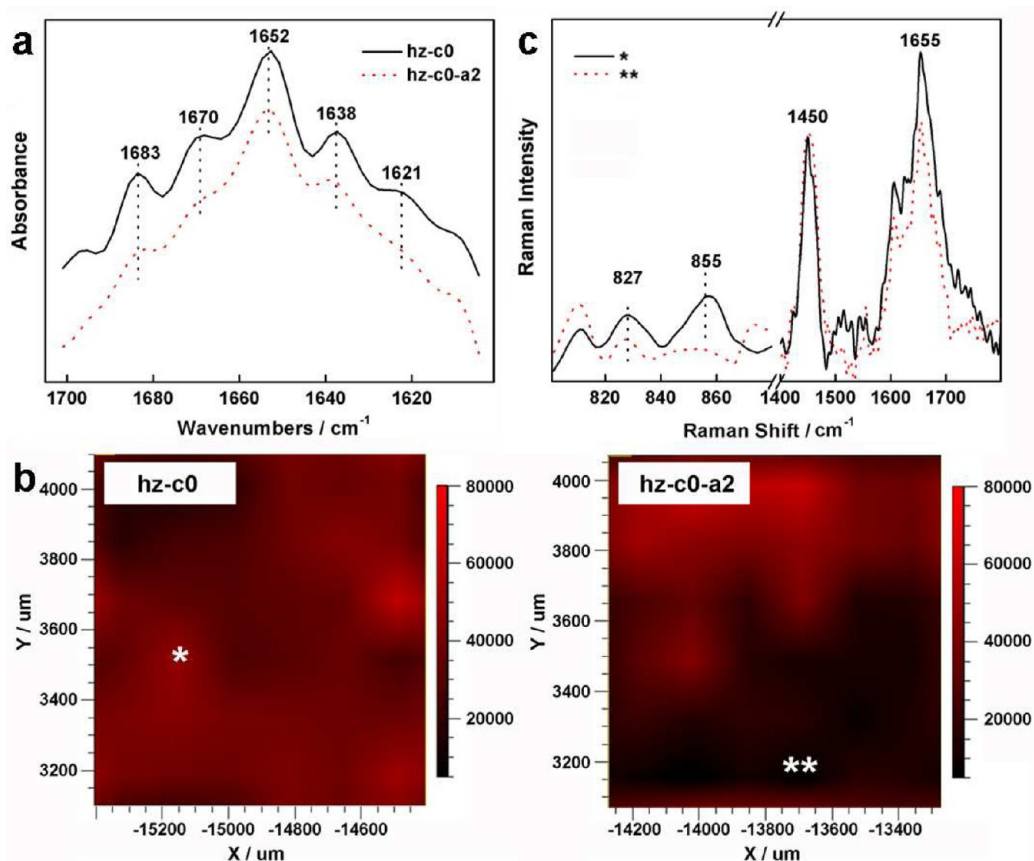
Figure 6. (a) Fourier-deconvoluted FTIR spectra of hz-c0 and hz-c0-a2; (b) confocal Raman images of hz-c0 and hz-c0-a2 mapping the signal intensity at 1670 cm^{-1}; and (c) individual Raman spectrum defined in the images as * and **.

gives rise to strong electron scattering from electron donor ligands, so OsO$_4$ is extensively used to stain unsaturated structures.[35] OsO$_4$ reacts with a hydrophobic double bond more than a hydrophilic carboxyl group, and has been recently used to indicate the periodic phase separation in nano-structured polymer particles.[35,36] Interestingly, black spots were present in the sections as shown in images c and d in Figure 5, and indicate that phase separation existed in prolamin protein composites. Similar spots were also observed in stained pure hordein fibers, but the color of pure hordein section was much lighter (figure not shown). These black spots could be the hydrophobic aggregated domains formed in prolamin protein networks. Therefore, the addition of zein particles may have facilitated the formation of certain special hydrophobic aggregated domains, acting as nanosized fillers to strengthen the assembled hordein/zein fibers, and then being easily stained by OsO$_4$. The size of these spots decreased radially from the center to the surface of the fiber. This reflects the uneven mobility of prolamin protein molecules induced by the stretching Coulombic force, where the reassembling of the outer layer was restricted to some extent. With the extra stretching force generated by the alignment, the phase separated structure was not obviously changed, but more tiny black spots were observed in the outer layer in some sections. This indicates that the alignment of electrospun fibers further promoted phase separation which may contribute to the observed improving fiber properties. The hydrophobic SCN did not alter the distribution of the aggregated domains, but could attach on them (Figure 5b), suggesting the hydrophobic nature of these black spots.

Fourier self-deconvolution to the amide I band (1600−1700 cm^{-1}) of hz-c0 and hz-c0-a2 is shown in Figure 6a in order to reveal the protein conformational changes in the electrospun fibers caused by uniaxial alignment. Fiber hz-c0 exhibited several bands which have been assigned to protein secondary structures: 1683 cm^{-1} (β-sheet), 1669 cm^{-1} (β-turn), 1652 cm^{-1} (α-helix), 1638 cm^{-1} (β-turn), and 1620 cm^{-1} (β-sheet).[33] The band at 1620 cm^{-1} was attributed to intermolecular β-sheet structure believed to be associated with the protein aggregation process.[37,38] During the preparation of electrospun assembled hordein/zein fibers, the original structure of hordein was initially unfolded in acetic acid, and then stretched in the presence of a strong Coulombic force during electrospinning to promote the formation of α-helical structure. On the other hand, the zein molecule built up a dense protein structure with its high α-helix content that could be well maintained in acetic acid, and then again in the nanofiber matrix. Therefore, the α-helix structure dominated the hordein/zein network with a strong absorption appearing at 1652 cm^{-1}. Several positions on the hz-c0-a2 fabric were examined. After the alignment, most positions exhibited similar secondary structures to those of hz-c0. However, some showed reduced structures, where the peak at 1652 cm^{-1} was almost maintained, but the intensity of other peaks obviously decreased. The reassembling of extended hordein molecules was partially prevented by the alignment process, whereas the structure of zein particles was likely to be unchanged. The uniaxial alignment generated extra stretching force on electro-spun protein fibers, promoting phase separation on one hand,

and reducing secondary structures of certain locations on the other.

Alignment-induced conformational changes of electrospun protein fibers were further investigated by confocal Raman imaging spectroscopy. Confocal Raman microscopy can be used as a simple, direct and noninvasive method to obtain a map of a sample area where the distinctive features are in the micrometer range. This becomes a useful tool to determine the secondary structure of protein and reveal local information regarding protein side groups.[39] Assignments of characteristic Raman bands were carried out based on previous studies, i.e., α-helix at 1655 ± 5 cm^{-1}, antiparallel β-sheet at 1670 ± 3 cm^{-1}, phenylalanine at 1000 cm^{-1}, and tyrosine at 850 and 830 cm^{-1}.[40] Confocal Raman images of hz-c0 and hz-c0-a2 mapping the signal intensity at 1670 cm^{-1} are shown in Figure 6b. In the large tested area (1 mm ×1 mm), the randomly oriented hz-c0 fabric exhibited a relatively uniform structure, whereas the uniaxial alignment caused the reduced β-sheet structure in some regions of hz-c0-a2. The individual spectrum in the areas with greatest and lowest signal intensity (defined as * and **) was compared in Figure 6c. Both of them had the amide I band centered at 1655 cm^{-1}, indicating the predominance of the α-helical structure. The intensity of amide I band decreased after the alignment, implying that the partially restricted rearrangement of extended hordein molecules and was in accordance with the result of FTIR. Specially, the tyrosine residues are sensitive to microenvironmental changes. The intensity ratio of the tyrosine ring vibrations at 850 and 830 cm^{-1} represents "buried" and "exposed" tyrosine residues, as well as the hydrogen bond of the phenol hydroxyl group.[25] If a tyrosine residue is on the surface of the protein, the phenolic OH will be simultaneously an acceptor and donor of moderate to weak hydrogen bonding, and the doublet intensity ratio ($I_{850/830}$) will be about 1:0.8 ($I = 1.25$). If the phenolic hydroxyl is the proton donor in a strong hydrogen bond, $I_{850/830}$ will be about 1:2 ($I = 0.5$).[41] As a result, $I_{855/827}$ in the area of the randomly oriented hz-c0 fabric was 1.69, suggesting that the tyrosine residues were mainly exposed and able to participate in moderate or weak hydrogen bonding.[42] At the meantime, the weak intensity of the Raman stretching at 855 cm^{-1} as compared to the Raman peak at 827 cm^{-1} ($I_{855/827} = 0.5$) implied that the tyrosine residues in hz-c0-a2 were buried and acted as strong hydrogen bond donors. This decrease of $I_{855/827}$ ratio revealed that the extra stretching force generated by the uniaxial alignment altered the distribution of tyrosine residues and induced stronger hydrogen bonding in the hz-c0-a2 fibers.

3.2. Hordein/Zein/SCN Fiber Properties. 3.2.1. Mechanical Properties.

The mechanical strength of electrospun hordein/zein/SCN fibers was particularly investigated in order to evaluate the reinforcing effects of both SCN and alignment. Typical stress–strain (σ-ε) curves of hz-c0, hz-c1, hz-c3, and hz-c5 are shown in Figure 7a. Fiber hz-c0 with an assembled hordein/zein structure promoted hydrophobic aggregated domains as nanosized fillers exhibited a tensile strength of 4.36 ± 0.29 MPa, much higher than that of electrospun pure hordein or zein fibers.[21] As expected, the tensile strength was further increased by incorporating SCN in hordein/zein network, which was 5.72 ± 0.14, 7.79 ± 0.36, and 7.52 ± 0.09 MPa for hz-c1, hz-c3, and hz-c5, respectively. The extent of the reinforcement of nanowhiskers depends on their dispersion in the matrix and the generation of a strong interaction between filler–filler and filler–matrix through physic-chemical bonding.[43] Moreover, the continuous percolat-
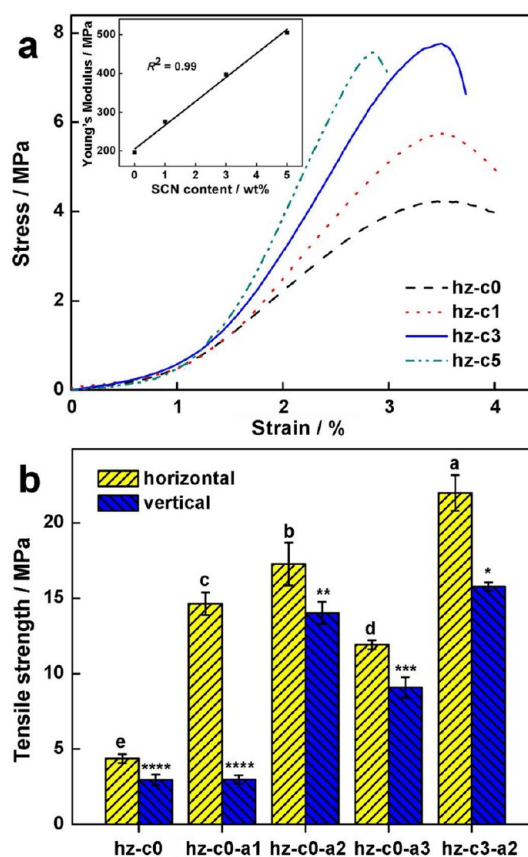
Figure 7. Mechanical properties of orientated electrospun hordein/zein/SCN fibers. Different symbols on the top of the columns indicate the significant difference ($p < 0.05$). Inset: Young's modulus with varying SCN contents.

ing network of rigid nanowhiskers forms through the matrix when their content reaches the percolation threshold (v_{Rc}), leading to a faster and uniform diffusion of stress.[16] The following relation has been observed between v_{Rc} and aspect ratio of rodlike particles[44]

$$v_{Rc} = 0.7/(L/d) \tag{3}$$

Calculated by using the density of SCN and protein as 1.60 and 1.35 g/cm^3,[31,45] the SCN content needed to form the percolating network in hordein/zein matrix was 2.94 wt %. With the surface modification by phenyltrimethylammonium chloride, SCN was well dispersed in the prolamin protein network. Therefore, for hz-c1, a small amount of SCN was uniformly inserted and wrapped in the assembled hordein/zein structure, resulting in improved strength without a significant impact on elongation. The percolating network subsequently formed in hz-c3 as shown by TEM, shows a result where the SCN content was just above the v_{Rc} value. This rigid filler network could support the fiber structure and facilitate the diffusion of stress. Thus, hz-c3 exhibited the increased tensile strength of 7.79 ± 0.36 MPa and retained elongation at break of about 3.50%, which was already obviously stronger than electrospun collagen/zein (6.30 MPa), silk fibroin (SF)/hydroxyapatite (1.17 MPa), SF/carbon nanotube (3.24 MPa), and poly(lactic acid)/CN (6.30 MPa) fibers.[7,46−48] With a further increase of SCN content, hz-c5 became brittle as reflected by the decreased tensile strength and elongation compared to those of hz-c3. This was because the SCN

network got denser and largely blocked the continuity of the protein matrix. There was a linear dependence of Young's modulus of electrospun hordein/zein/SCN fibers on the amount of SCN, confirming the uniform dispersion of SCN even at high concentration.

Interestingly, the mechanical properties of electrospun composite fabrics were closely related to the orientation of fibers. As shown in Figure 7b, the tensile strength in both tangential and normal directions was evaluated. In our preliminary experiment, the handling properties of single-layered uniaxially aligned fibers was poor explained by the lack of connections in the normal direction, so three kinds of electrospun fabrics were prepared by combining different orientated layers together. Fiber hz-c0 exhibited similar tensile strength in both tested directions because of the randomly orientated pattern. For hz-c0-a1, which was composed of one layer of uniaxially aligned fibers and one layer of random fibers, the tensile strength in tangential direction was greatly increased, while that in normal direction was as same as hz-c0. This indicates that the alignment of fibers could significantly improve the mechanical property in one direction. With the alignment in both directions, hz-c0-a2 showed a dramatically reinforced mechanical property with tensile strength of 17.26 ± 1.41 and 14.02 ± 0.74 MPa in tangential and normal directions, respectively. The second aligned layer tightly bound up the first one due to the force generated by high-speed rotating drum, leading to the higher tensile strength in the tangential direction. Fiber hz-c0-a2 was thus significantly stronger than not only hz-c0, but also uniaxially aligned poly(L-lactide)/poly(ε-caprolactone)/carbon nanotube (4.34 MPa) and poly(vinyl alcohol)/CN (10.50 MPa) fibers.[19,49] However, hz-c0-a3 with three different orientated layers exhibited a decreased strength. It indicated that the mechanical properties of electrospun prolamin protein fibers mainly depended on the proportion of aligned fibers rather than the combination of different layers. The alignment in one aspect parallel piled up the fibers in same direction to diffuse the stress. In another, the partial phase separation of prolamin proteins increased the hydrophobic fillers and induced conformational change of proteins to form stronger hydrogen bonds, resulting in reinforced mechanical properties. With the addition of 3 wt % SCN, the tensile strength of hz-c3-a2 was further increased to 21.99 ± 1.19 and 15.78 ± 0.27 MPa, even higher than the mechanical properties of cancellous bones (strength of 5−10 MPa and modulus of 50−100 MPa),[50] suggesting the potential use as tissue scaffold. Therefore, both SCN and alignment had a tremendous effect on improving the mechanical properties of electrospun hordein/zein fibers.

3.2.2. Stability. TGA measurement for orientated hordein/zein/SCN fibers is shown in Figure 8 to evaluate the stability of network structure. The thermal degradation of biopolymers usually involves two steps: the initial stage was related to the degradation of the biopolymer network which was followed by the degradation of the inner covalent bonds of the biopolymer monomers.[51] Thus, the initial weight loss temperature of the samples was investigated and compared. With the addition of 3 wt % SCN, an increased weight loss of hordein/zein/SCN fibers was observed in the first step compared to that of hz-c0, indicating that the thermal resistance of prolamin protein matrix was reduced. The formation of continuous SCN network may block the combination of protein molecules to some extent. Interestingly, the aligned fibers, with or without SCN, exhibited an improved thermal stability which only
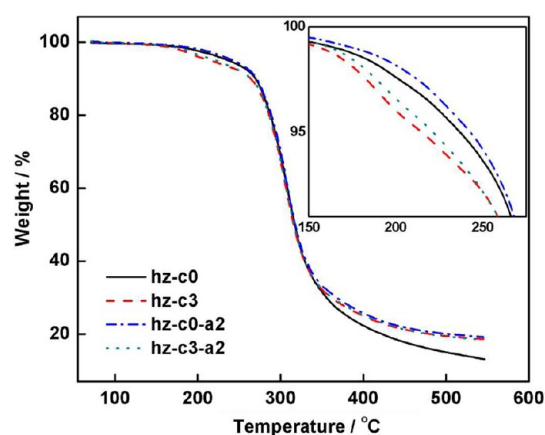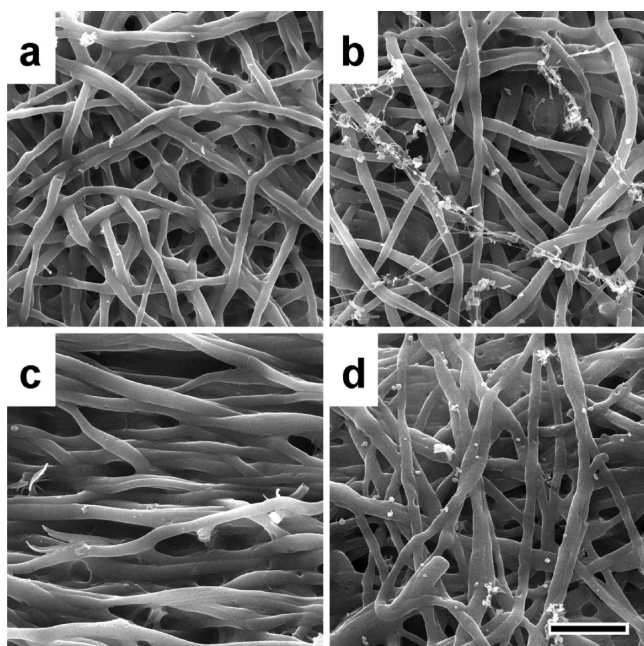

Figure 8. TGA curves of orientated electrospun hordein/zein/SCN fibers.

depended on the inner structure of fibers rather than their piling up pattern. As revealed by TEM results, the alignment further promoted a phase separation of prolamin proteins. More tiny aggregated domains were created by the extra stretching force and acted as nanosized hydrophobic fillers to stabilize the hordein/zein matrix. At the same time, the rearrangement of protein structure was partially hindered where the phenol hydroxyl groups were buried into the intermolecular interface to form strong hydrogen bonds as shown in FTIR and Raman spectra. These alterations induced by uniaxial alignment were proved to reinforce the mechanical properties and thermal stability of electrospun hordein/zein/SCN fibers.

Excessive swelling of electrospun protein fibers in aqueous media is another problem that limits their applications. Thus the morphology of orientated hordein/zein/SCN fibers after the treatment with water for 24 h at room temperature was investigated to evaluate water resistance of modified fibers (as shown in Figure 9). The diameter distribution of swollen fibers is summarized in Figure 4b and Table 2. The whole electrospun fabric underwent shrinking to certain extent while the fibers themselves swelled after the treatment. Because both hydrophobic and hydrophilic components existed in the fiber network, this shrinkage was probably due to the aggregating tendency of nanosized hydrophobic domains. The d_n value of hz-c0 increased to 1.55 times. This swelling degree was lower than not only pure hordein fibers but also cross-linked PVA/hyaluronic acid (HA) fibers.[52] With the addition of SCN, the swelling of prolamin protein matrix was significantly restricted and the d_n value of hz-c5 only increased to 1.18 times, which was even lower than that of SF/HA/polycaprolactone (PCL) fibers.[53] However, the swelling ratio of fibers, with or without the uniaxial alignment, was similar, because the fiber structure was only partially altered and the average diameter was slightly changed. The aligned hordein/zein/SCN fabrics exhibited the well-designed 3D porous structure in water which maintained the large surface area to volume ratio and excellent pore-interconnectivity. This could allow quick response to signaling pathways and facilitate the transportation of bioactive compounds in biomedical, pharmaceutical and nutraceutical applications. The presence of SCN and alignment regulated the diameter of wet fibers and 3D pattern of fabric network, respectively. Moreover, the total volume and P_d values of these electrospun fabrics did not increase after the water treatment, suggesting that when implanted in the body, these fabrics
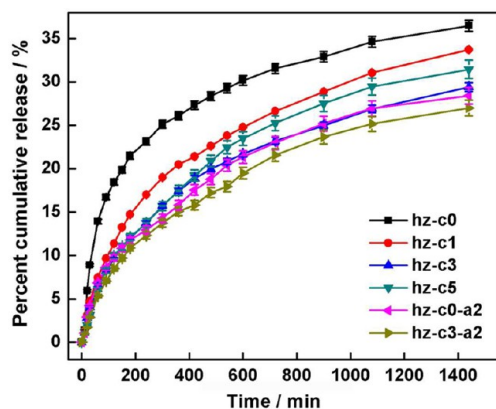
Figure 9. SEM images of orientated electrospun hordein/zein/SCN fibers immersed in water for 24 h: (a) hz-c0, (b) hz-c5, (c) hz-c0-a2, and (d) hz-c3-a2. Scale bar: 10 μm.

would not excessively or irregularly swell and cause any physical or mechanical hindrance to the surrounding tissues.[54]

3.2.3. Release Behavior. The release behavior of electrospun hordein/zein/SCN fibers was subsequently investigated in PBS at 37 °C to simulate a body fluid system. Riboflavin was employed as a model bioactive molecule. As shown in Figure 10, moderate release rate was observed for hz-c0 and 36.48%

Figure 10. Release profiles of riboflavin from drug-loaded orientated electrospun hordein/zein/SCN fibers in PBS at 37 °C.

riboflavin was detected in the buffer after 24 h. This was due to the well-maintained 3D porous structure in PBS which could provide a controlled release. Interestingly, the accumulative release of riboflavin from hz-c3 and hz-c0-a2 was 29.41 and 28.40%, respectively, indicating that both SCN and alignment obviously decreased the release rate. The Korsmeyer-Peppas semiempirical equation was then applied to explore the mechanism of riboflavin release from electronspun fibers[55]

$$M_t/M_\infty = kt^n \tag{4}$$

where M_t/M_∞ is the fraction of model molecule released after time t relative to the amount of model molecule released at infinite time, k is a constant and n is the diffusional exponent. Inferences about the release mechanism are based on the fit of this equation to the model molecule release data through 60% dissolution and comparison of the value of n to the semiempirical values for slab geometry reported by Peppas. Riboflavin release from all the samples displayed a typical sigmoid profile with n values first in the range of 0.54−0.77 (R^2 = 0.989−0.999) and then 0.30−0.45 (R^2 = 0.986−0.997). Enhanced riboflavin diffusion occurred due to the swelling of orientated hordein/zein/SCN fibers in PBS. When the swelling reached the equilibrium, the release followed a diffusion-controlled mechanism. According to the results of water resistance test, the addition of SCN and alignment of fibers affected the release behaviors in different ways. With the increase of SCN content from 0 to 3 wt %, the assembled hordein/zein matrix was reinforced by the formation of SCN percolating network, which restricted the swelling of matrix and thus slowed down the diffusion of riboflavin. When the SCN content was 5 wt %, the continuity of hordein matrix was blocked to some extent, so the diffusion within the fiber was facilitated, leading to the accelerated release after 6 h. Although the alignment did not significantly change the swelling ratio of electrospun fibers, the parallel placed swollen fibers may hinder the permeation of PBS solution, so as to slow riboflavin dissolving and leaching out. By applying these two modifications at the same time, hz-c3-a2 exhibited the lowest release rate and only 26.99% of the loaded riboflavin was detected after 24 h. Therefore, both SCN and alignment could improve the controlled release by effectively reducing the "burst effect" by changing the swollen status of composite fibers.

4. CONCLUSION

Electrospun prolamin protein fabrics with greatly improved mechanical properties were successfully prepared by the incorporation of SCN and controlled alignment of fibers. The surface modified nanowhiskers were uniformly dispersed in the hordein/zein matrix and a percolating network of these rigid fillers subsequently formed to facilitate a faster diffusion of stress when the SCN content reached 3 wt %. However, further addition of SCN blocked the continuity of hordein and resulted in the brittle fibers with a decreased tensile strength and elongation at break. The high-speed rotating drum collector was used to apply an extra stretching force on electrospun fibers to pile them up in parallel. This also promoted the phase separation of prolamin proteins, generated more tiny hydrophobic domains to stabilize the fibers, and induced conformational changes of proteins to form stronger hydrogen bonds. Electrospun hordein/zein/SCN fabrics composed of different orientated layers were obtained, and their mechanical properties were mainly related to the proportion of aligned fibers. Fiber hz-c3-a2 exhibited the highest tensile strength of 21.99 ± 1.19 and 15.78 ± 0.27 MPa in tangential and normal directions, respectively, which was 4.04 and 4.35 times stronger than that of original hordein/zein fibers. Moreover, the water resistance of SCN reinforced fibers was improved and wet aligned fibers kept their regulated 3D pattern. These changes could slow down the permeation of PBS solution and diffusion of riboflavin, leading to a decreased "burst effect" and a better controlled release of loaded bioactive compounds. These orientated electrospun hordein/zein/SCN fibers are expected to expand the application of prolamin protein fabrics, and have

the potential to be used as wound healing materials, tissue scaffolds and delivery systems of bioactive molecules.

■ AUTHOR INFORMATION

Corresponding Author

*E-mail: lingyun.chen@ualberta.ca. Tel.: +1-780-492-0038. Fax: +1-780-492-8914.

Notes

The authors declare no competing financial interest.

■ REFERENCES

(1) Yang, H.; Hong, W.; Dong, L. *Appl. Phys. Lett.* **2012**, *100*, 153510.

(2) Yohe, S. T.; Colson, Y. L.; Grinstaff, M. W. *J. Am. Chem. Soc.* **2012**, *134*, 2016−2019.

(3) Wei, Q.; Tao, D.; Xu, Y. In *Functional Nanofibers and Their Applications*; Wei, Q., Ed.; Woodhead Publishing Limited: Cambridge, U.K., 2012; p 3−21.

(4) Scheibel, T. *Curr. Opin. Biotechnol.* **2005**, *16*, 427−433.

(5) Zhang, F.; Zuo, B.; Fan, Z.; Xie, Z.; Lu, Q.; Zhang, X.; Kaplan, D. L. *Biomacromolecules* **2012**, *13*, 798−804.

(6) Jiang, Q.; Reddy, N.; Yang, Y. *Acta Biomater.* **2010**, *6*, 4042−4051.

(7) Pan, H.; Zhang, Y.; Hang, Y.; Shao, H.; Hu, X.; Xu, Y.; Feng, C. *Biomacromolecules* **2012**, *13*, 2859−2867.

(8) Selling, G. W.; Woods, K. K.; Biswas, A. *J. Appl. Polym. Sci.* **2012**, *123*, 2651−2661.

(9) Selling, G. W.; Biswas, A.; Patel, A.; Walls, D. J.; Dunlap, C.; Wei, Y. *Macromol. Chem. Phys.* **2007**, *208*, 1002−1010.

(10) Habibi, Y.; Goffin, A. L.; Schiltz, N.; Duquesne, E.; Dubois, P.; Dufresne, A. *J. Mater. Chem.* **2008**, *18*, 5002−5010.

(11) Yang, H.; Tejado, A.; Alam, N.; Antal, M.; van de Ven, T. G. M. *Langmuir* **2012**, *28*, 7834−7842.

(12) Salajková, M.; Berglund, L. A.; Zhou, Q. *J. Mater. Chem.* **2012**, *22*, 19798−19805.

(13) Sturcova, A.; Davies, G. R.; Eichhorn, S. J. *Biomacromolecules* **2005**, *6*, 1055−1061.

(14) Capadona, J. R.; Shanmuganathan, K.; Trittschuh, S.; Seidel, S.; Rowan, S. J.; Weder, C. *Biomacromolecules* **2009**, *10*, 712−716.

(15) Wang, Y.; Cao, X.; Zhang, L. *Macromol. Biosci.* **2006**, *6*, 524−531.

(16) Wang, Y.; Chen, L. *Carbohydr. Polym.* **2011**, *83*, 1937−1946.

(17) Park, D. J.; Choi, Y.; Heo, S.; Cho, S. Y.; Jin, H. J. *J. Nanosci. Nanotechnol.* **2012**, *12*, 6139−6144.

(18) Ravandi, S. A. H.; Sadrjahani, M. *J. Appl. Polym. Sci.* **2012**, *124*, 3529−3537.

(19) Lee, J.; Deng, Y. *Macromol. Res.* **2012**, *20*, 76−83.

(20) Liao, C.; Wang, C.; Shih, K.; Chen, C. *Eur. Polym. J.* **2011**, *47*, 911−924.

(21) Wang, Y.; Chen, L. *J. Mater. Chem.* **2012**, *22*, 21592−21601.

(22) Wang, C.; Tian, Z.; Chen, L.; Temelli, F.; Liu, H.; Wang, Y. *Cereal Chem.* **2010**, *87*, 597−606.

(23) van de Ven, T. G. M.; Tejado, A.; Alam, M. N.; Antal, M. *Novel highly charged non-water soluble cellulose products, includes all types of cellulose nanostructures especially cellulose nanofibers, and method of making them.* U.S. Provisional Patent Application 3776923-v3, 2011.

(24) Silva, S. S.; Maniglio, D.; Motta, A.; Mano, J. F.; Reis, R. L.; Migliaresi, C. *Macromol. Biosci.* **2008**, *8*, 766−774.

(25) Guo, Y.; Cai, W.; Tu, K.; Tu, S.; Wang, S.; Zhu, X.; Zhang, W. *J. Agric. Food Chem.* **2013**, *61*, 185−192.

(26) Stephens, J. S.; Fahnestock, S. R.; Farmer, R. S.; Kiick, K. L.; Chase, D. B.; Rabolt, J. F. *Biomacromolecules* **2005**, *6*, 1405−1413.

(27) Kuzuhara, A. *J. Mol. Struct.* **2013**, *1047*, 186−193.

(28) Selling, G. W.; Woods, K. K.; Biswas, A. *Polym. Int.* **2011**, *60*, 537−542.

(29) Chazeau, L.; Paillet, M.; Cavaillé, J. Y. *J. Polym. Sci., Part B: Polym. Phys.* **1999**, *37*, 2151−2164.

(30) Boluk, Y.; Zhao, L.; Incani, V. *Langmuir* **2012**, *28*, 6114−6123.

(31) Sun, C. *J. Pharm. Sci.* **2005**, *94*, 2132−2134.

(32) Elazzouzi-Hafraoui, S.; Nishiyama, Y.; Putaux, J.; Heux, L.; Dubreuil, F.; Rochas, C. *Biomacromolecules* **2008**, *9*, 57−65.

(33) Wang, Y.; Chen, L. *Macromol. Mater. Eng.* **2012**, *297*, 902−913.

(34) Bals, S.; Kabius, B.; Haider, M.; Radmilovic, V.; Kisielowski, C. *Solid State Commun.* **2004**, *130*, 675−680.

(35) Belazi, D.; Solé-Domènech, S.; Johansson, B.; Schalling, M.; Sjövall, P. *Histochem. Cell Biol.* **2009**, *132*, 105−115.

(36) Higuchi, T.; Tajima, A.; Motoyoshi, K.; Yabu, H.; Shimomura, M. *Angew. Chem., Int. Ed.* **2009**, *48*, 5125−5128.

(37) Secundo, F.; Guerrieri, N. *J. Agric. Food Chem.* **2005**, *53*, 1757−1764.

(38) Jackson, M.; Mantsch, H. H. *Can. J. Chem.* **1991**, *69*, 1639−1642.

(39) Fernandez, A.; Torres-Giner, S.; Lagaron, J. M. *Food Hydrocolloids* **2009**, *23*, 1427−1432.

(40) Georget, D. M. R.; Barker, S. A.; Belton, P. S. *Eur. J. Pharm. Biopharm.* **2008**, *69*, 718−726.

(41) Hsu, B.; Weng, Y.; Liao, Y.; Chen, W. *J. Agric. Food Chem.* **2005**, *53*, 5089−5095.

(42) Liu, R.; Zhao, S.; Xie, B.; Xiong, S. *Food Hydrocolloids* **2011**, *25*, 898−906.

(43) Wang, Y.; Zhang, L. *J. Nanosci. Nanotechnol.* **2008**, *8*, 5831−5838.

(44) Azizi Samir, M. A. S.; Alloin, F.; Dufresne, A. *Biomacromolecules* **2005**, *6*, 612−626.

(45) Fischer, H.; Polikarpov, I.; Craievich, A. F. *Protein Sci.* **2004**, *13*, 2825−2828.

(46) Lin, J.; Li, C.; Zhao, Y.; Hu, J.; Zhang, L. *ACS Appl. Mater. Interfaces* **2012**, *4*, 1050−1057.

(47) Ming, J.; Zuo, B. *Mater. Chem. Phys.* **2012**, *137*, 421−427.

(48) Shi, Q.; Zhou, C.; Yue, Y.; Guo, W.; Wu, Y.; Wu, Q. *Carbohydr. Polym.* **2012**, *90*, 301−308.

(49) Liao, G.; Zhou, X.; Chen, L.; Zeng, X.; Xie, X.; Mai, Y. *Compos. Sci. Technol.* **2012**, *72*, 248−255.

(50) Katsanevakis, E.; Wen, X.; Zhang, N. *Adv. Polym. Sci.* **2012**, *246*, 63−100.

(51) Torres-Giner, S.; Lagaron, J. M. *J. Appl. Polym. Sci.* **2010**, *118*, 778−789.

(52) Kim, K.; Akada, Y.; Kai, W.; Kim, B.; Kim, I. *J. Biomater. Nanobiotechnol.* **2011**, *2*, 353−360.

(53) Li, L.; Qian, Y.; Jiang, C.; Lv, Y.; Liu, W.; Zhong, L.; Cai, K.; Li, S.; Yang, L. *Biomaterials* **2012**, *33*, 3428−3445.

(54) Kasoju, N.; Bora, U. *Biomed. Mater.* **2012**, *7*, 045004.

(55) Chen, L.; Remondetto, G.; Rouabhia, M.; Subirade, M. *Biomaterials* **2008**, *29*, 3750−3756.